Thrombosis Research 126 (2010) 137–143

Contents lists available at ScienceDirect

Thrombosis Research

journal homepage: www.elsevier.com/locate/thromres

Regular Article

Microscopic clot fragment evidence of biochemo-mechanical degradation effects in thrombolysis

Franci Bajd [a], Jernej Vidmar [b], Aleš Blinc [c], Igor Serša [a,*]

[a] Jožef Stefan Institute, Jamova 39, Ljubljana 1000, Slovenia
[b] Institute of Physiology, Medical Faculty, University of Ljubljana, Zaloška 4, Ljubljana 1000, Slovenia
[c] Department of Vascular Diseases, University of Ljubljana Medical Centre, Zaloška 7, Ljubljana 1525, Slovenia

ARTICLE INFO

Article history:
Received 11 February 2010
Received in revised form 22 April 2010
Accepted 23 April 2010
Available online 23 May 2010

Keywords:
Thrombolysis
Thrombolytic agents
Rheology
Optical microscopy

ABSTRACT

Introduction: Although fibrinolytic treatment has been used for decades, the interactions between the biochemical mechanisms and the mechanical forces of the streaming blood remain incompletely understood. Analysis of the blood clot surface *in vitro* was employed to study the concomitant effect of blood plasma flow and recombinant tissue plasminogen activator (rt-PA) on the degradation of retracted, non-occlusive blood clots. Our hypothesis was that a faster tangential plasma flow removed larger fragments and resulted in faster overall thrombolysis.

Materials and Methods: Retracted model blood clots were prepared in an optical microscopy chamber and connected to an artificial perfusion system with either no-flow, or plasma flow with a velocity of 3 cm/s or 30 cm/s with or without added rt-PA at 2 μg/ml. The clot surface was dynamically imaged by an optical microscope for 30 min with 15 s intervals.

Results: The clot fragments removed during rt-PA mediated thrombolysis ranged in size from that of a single red blood cell to large agglomerates composed of more than a thousand red blood cells bound together by partly degraded fibrin. The average and the largest discrete clot area change between images in adjacent time frames were significantly higher with the faster flow than with the slow flow (14,000 μm^2 and 160,000 μm^2 vs. 2200 μm^2 and 10,600 μm^2).

Conclusions: On the micrometer scale, thrombolysis consists of sequential removal of clot fragments from the clot surface. With increasing tangential plasma flow velocity, the size of the clot fragments and the overall rate of thrombolysis increases.

Introduction

Formation of intravascular blood clots is an important component of venous thromboembolism [1] and of the final stages of atherothrombosis that may, depending on the affected vascular bed, cause acute coronary syndrome, ischemic cerebrovascular stroke [2,3], or critical limb ischemia [4]. Thrombotic disorders may be treated by thrombolytic therapy with plasminogen activators that convert the inactive proenzyme plasminogen into the active serine protease plasmin which in turn degrades the fibrin meshwork [5]. Although thrombolytic therapy has been used for decades, the interactions of its biochemical mechanisms with the mechanical forces of streaming blood remain incompletely understood.

Experimental studies and mathematical models have been published on dissolution of non-occlusive blood clots with emphasis on the dynamics of the thrombolytic biochemical reactions [6–10], or on the mechanical effects of the streaming blood on clot degradation [6,8,11]. A common finding of these studies is that fast tangentially directed blood flow along a non-occlusive blood clot accelerates thrombolysis. The proposed mechanisms of tangential blood flow are to increase the delivery of the thrombolytic agent into the blood clot and to exert large mechanical forces on the clot surface due to blood viscosity or turbulence [11–13]. Additionally, it was reported that, in comparison to non-retracted blood clots, retracted ones are less susceptible to thrombolysis due to syneresed serum from their porous interior [13–15]. All of the above mentioned experimental studies employed either an artificial perfusion system combined with a macroscopic imaging technique (MRI, conventional photography …) or were done in the absence of flow (static conditions) and employed microscopic imaging (conventional optical and confocal microscopy). Few studies combined perfusion experiments with microscopic imaging [7]. However, none of the studies was focused on the analysis of clot degradation products in relation to the velocity of tangential blood plasma flow.

Our previous studies have shown that flow enhances thrombolysis to a degree that cannot be ascribed only to promotion of biochemical clot degradation [6,15]. We hypothesized that with faster tangential flow, resulting in stronger shear forces of the streaming plasma, the fragments removed from the clot surface would be larger, albeit

Abbreviations: RBC, red blood cell; rt-PA, recombinant tissue plasminogen activator.

* Corresponding author. Fax: +386 1 477 3696.
E-mail address: igor.sersa@ijs.si (I. Serša).

0049-3848/$ – see front matter © 2010 Elsevier Ltd. All rights reserved.
doi:10.1016/j.thromres.2010.04.012

incompletely biochemically degraded. The aim of this study was to test this hypothesis by optical microscopy of the surface of retracted model blood clots in an artificial perfusion system.

Materials and methods

Model blood clots

Whole-blood was collected from the cubital veins of healthy volunteers, who showed no evidence of coagulation disorders or acute illness. Blood was drawn under standardized conditions into 4.5 ml-vials (Vacuntainer, Becton-Dickinson, Germany) containing 0.45 ml of 0.129 mol/l Na-citrate. To neutralize the anticoagulation effect of Na-citrate, 50 µl of $CaCl_2$ at a concentration of 2 mol/l, was added to the collected blood samples. Clotting was initiated by adding 100 µl/ml of thrombin (Thrombin, Sigma, Germany) to a final concentration of 1.37 NIH unit/ml. This was followed by the injection of 25 µl of the mixture into a chamber, designed for observation by optical microscopy (Fig. 1A). The observation chamber, which was made of microscopy slides, was 25 mm long (dimension along the flow direction), 5 mm wide and 1 mm high. To obtain clots with a gradually decreasing thickness, i.e., a triangular profile, clotting was performed in an observation chamber tilted 30° along the axis parallel to the longest side of the chamber. The adherence of the clot to the chamber side wall was assured by coating the wall with an epoxy two-component glue (Uhu, Germany) (Fig. 1B). The glue did not interfere with clotting or thrombolysis. A similar type of glue was used for attaching clots to the perfusion system in our previous work without marked interference with thrombolysis [15]. The blood mixture in the chamber was incubated for two hours at room temperature (24 °C) to allow for complete formation of the fibrin meshwork and for spontaneous clot retraction. After the incubation, the initial wedge-shape of blood clot was slightly deformed due to surface tension and clot retraction. Each clot in the study was prepared in a new, identically designed observation chamber.

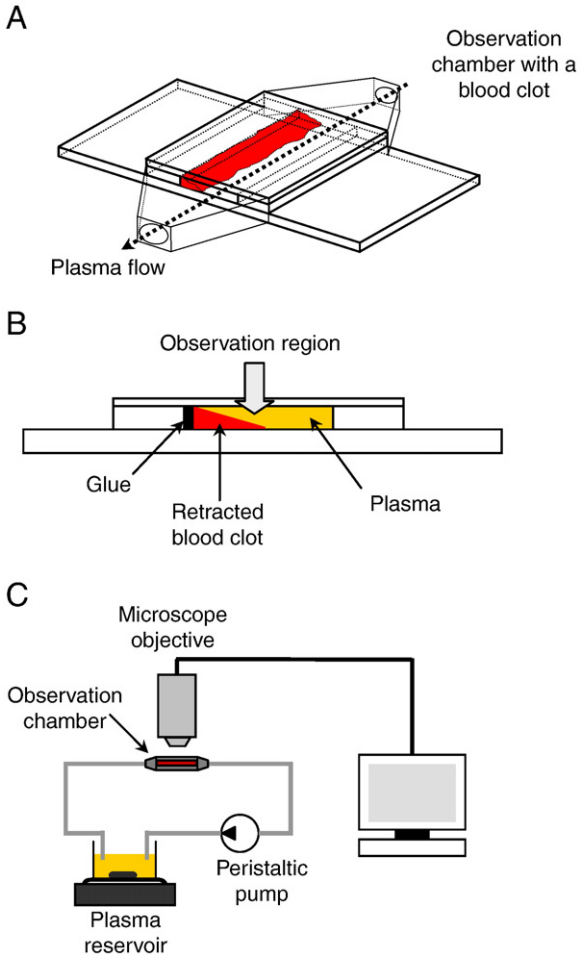

Fig. 1. Optical microscopy of thrombolysis was performed with a model retracted whole-blood clot tightly sealed in the observation chamber (A). A cross-section through the chamber (B) shows the chamber composition; a thin layer of the wedge-shaped blood clot and flowing plasma above it. The chamber was connected to the perfusion system and placed under the optical microscope equipped with a digital camera (C).

Conditions of thrombolysis

The clot filled 20% of the chamber volume while 80% of the volume was available for plasma flow. Cone shaped, 5 mm long plastic inserts were glued by an epoxy two-component glue to the proximal and distal sides of the observation chamber and connected at both ends to a flexible plastic hose of 3 mm inner diameter. The inserts were needed to transform the flow profile from the cylindrical geometry in the hose to the planar geometry in the chamber. The 1 m long hose connected the observation chamber to a peristaltic pump (913 Mityflex, Germany) in a thermoregulated (36 °C) reservoir containing 40 ml of human plasma of a matching AB0 blood group (Fig. 1C). Fresh frozen plasma was obtained from the Blood Transfusion Centre of the Republic of Slovenia that processes exclusively blood donated by volunteers who pass the clinical and laboratory health standards and do not take medication. Plasma from single donors was packed in bags of approximately 250 ml. Prior to dissolution experiments the frozen plasma contained in a single bag was thawed and used in six individual experiments. In total plasma of five different donors was distributed between 30 experiments. Each experiment started with an initial perfusion of the clot, prior to thrombolysis, for 15 min at a flow rate of 0.15 ml/s in order to remove any possible debris weakly attached to the clot surface. Perfusion was continued for an additional 30 min in one of the six different experimental regimes: non-perfusion, slow perfusion (volume flow of 0.15 ml/s with a velocity of 3 cm/s) and faster perfusion (volume flow of 1.5 ml/s with a velocity of 30 cm/s) all with or without the thrombolytic agent. Recombinant tissue plasminogen activator - rt-PA (Actilyse, Boehringer, Germany) was used at a concentration of 2 µg/ml, which corresponds to the expected plasma concentration in an average-sized person after injection of a 10 mg rt-PA bolus, i.e., during treatment of acute myocardial infarction [16]. At least five experiments were performed for each of the six experimental regimes.

Optical microscopy

Clots were imaged by a Nikon 80i Eclipse optical microscope equipped with a Nikon 10x Plan Fluor objective (numerical aperture 0.3, working distance 16 mm) and a high-resolution CCD camera (Nikon DS-Fi1). The optical system was controlled by the Nikon NIS Elements software package. Digital images were recorded dynamically at 15 s intervals (0.07 fps) with a 20 ms exposure time during continuous flow of plasma through the chamber. The imaging matrix was 640×480 with an in-plane resolution of 1.3 µm per pixel that yielded a field of view (FOV) of 832×624 µm. The optical microscopy settings represented the best compromise between the relatively large FOV and the resolution needed for detection of single whole-blood cells and larger clot degradation products. The FOV was positioned above the border between the clot and the glass. Initially, approximately 90% of the FOV was covered by the thin clot region with flowing plasma above.

Image analysis

To obtain clot dissolution curves (normalized non-lysed blood clot area as a function of time) and to obtain the size distribution of

discrete clot area changes between images taken at 15 s intervals, dynamically acquired image sets were quantitatively analyzed by the ImageJ program (NIH, USA). First, images were converted into an 8-bit grey scale (with a range of values between 0 and 255) in which the intensity of plasma corresponded to a value of 150 ± 15, while intensities below 90 corresponded to the blood clot and fragments removed from it. Therefore, for each image in the sequence, the clot area was determined using the threshold value of 90. The non-lysed clot areas obtained in this way were then corrected by adding the area equal to the difference between the FOV area and the initial clot area (typically 90% of the FOV) and then normalized to the FOV area. In addition, derivatives of clot dissolution curves, i.e., the differences between sequential non-lysed clot areas, were calculated to obtain a sequence of clot degradation events. Removed clot area within a degradation event corresponds to the sum of the areas of clot fragments removed in a 15 s interval. The area serves also as an estimate of the upper limit of the clot fragment area removed. The degradation events of all experiments belonging to the same flow and thrombolytic regime were sorted by their areas in bins of 1000 μm^2 to obtain an area change distribution, i.e., a distribution of the frequency of degradation events as function of their area. The area change distributions thus obtained were then normalized to the total number of degradation events.

The graph can be understood as a time sequence of clot degradation events, i.e., it depicts areas of the removed clot fragments within 15 s time intervals. Two such distributions, one for slow flow and the other for faster flow (both with thrombolytic agent rt-PA), are shown in Fig. 5.

Statistical analysis

The two tailed Student's t-test was used for comparing two sets of data with unequal variance, i.e. the normalized non-lysed blood clot areas in two different flow regimes at a given time. Distributions of discrete clot area changes for slow and faster flow were analyzed by the Mann-Whitney test. Descriptive statistics were given as means $\pm$ standard deviations. All analyses were done by the Origin (OriginLab Corporation, Northampton MA, USA) software package.

Results

Dynamical optical microscopy of thrombolysis

Three representative experiments with corresponding sets of dynamically recorded optical microscopy images, two recorded during rt-PA mediated thrombolysis with slow flow at 3 cm/s and the other during thrombolysis with faster flow at 30 cm/s are shown in Fig. 2A, B (slow flow) and 2C (faster flow). With slow flow, thrombolysis was much slower than with faster flow. This is quite apparent from comparison of clot area reduction in parallel time

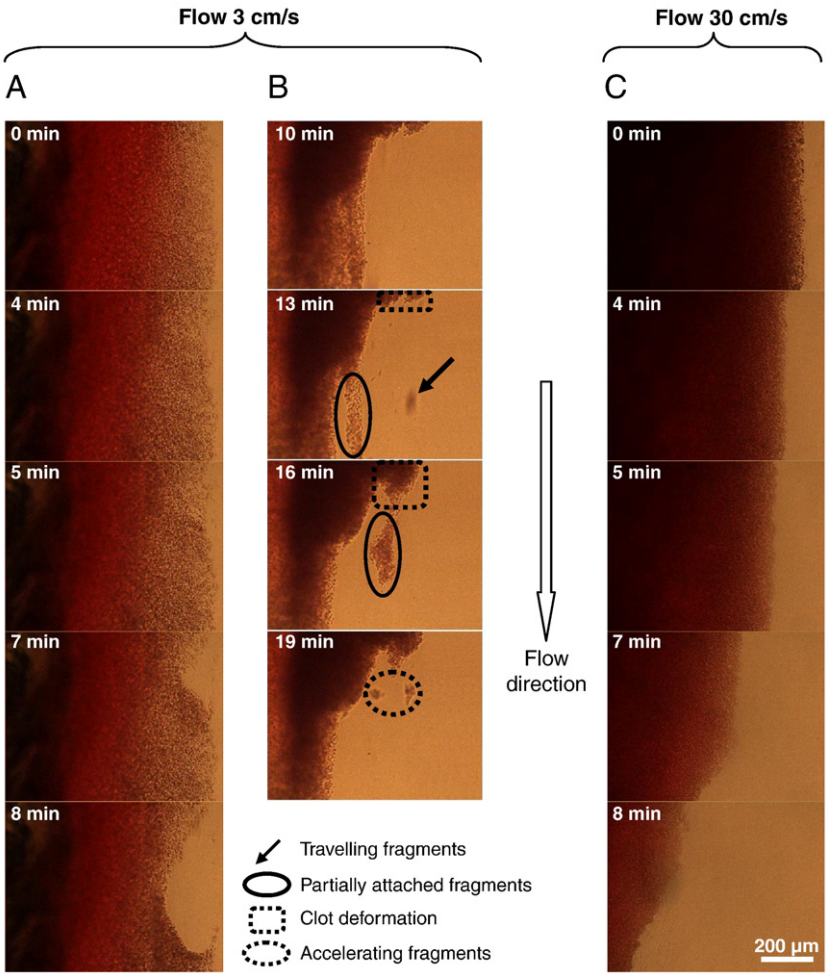

Fig. 2. Three experiments of thrombolysis of retracted whole-blood clots followed by optical microscopy: two with slow (A, B) and one with faster (C) plasma flow with corresponding velocities of 3 cm/s and 30 cm/s. Regions encircled by a solid line denote weakly attached clot fragments that were or are about to be removed from the clot surface, while the regions marked by a dotted line denote parts of the clot that were bent in the direction of flow. The black arrow indicates an accelerating and therefore blurred clot fragment that is flowing with the plasma.

frames (0 - 8 min) of Fig. 2A and C; in the last frame of the slow flow experiment (Fig. 2A, 8 min) 83% of FOV was still covered with the clot, while in the last frame of the faster flow experiment (Fig. 2C, 8 min) clot FOV coverage was only 27%. In slow flow most interesting dissolution events start occurring after 10 min of thrombolysis beginning, when in faster flow most clots are practically completely dissolved. In the slow flow experiment in Fig. 2B (10 - 19 min) it was possible to follow the removal of individual clot fragments. The encircled areas in the image sequence in Fig. 2B (frames at 13 and 16 min) show regions of the clot that were removed from the bulk of the clot in the next frame. The removed fragments varied in size from that of a few RBCs (Fig. 2B, 19 min) to large RBC agglomerates more than 200 μm in length (Fig. 2B, 13 and 16 min). In some cases, prior to removal the fragment was bent in the direction of flow (dotted curved region in Fig. 2B). Fragments of the clot that were removed from the clot upstream of the FOV and travelled with the velocity of the plasma flow (i.e., terminal velocity) could not be detected in the microscopy images. This is because the fragments traversed the FOV in a time that was approximately equal (with slow flow) or significantly shorter (with faster flow) than the frame exposure time, and their images were therefore completely blurred. Only those fragments that were removed within the FOV and had not yet accelerated to the terminal velocity were detected (Fig. 2B, 13 min, black arrow indicates fragment). With the faster flow, detection of removed fragments was much harder due to their faster acceleration. This explains why no removed clot fragments were seen in any of the frames in Fig. 2C. However, the clot degradation process could still be monitored by observing the remaining clot. With the faster flow, much larger fragments of the clot were removed from the clot than with slow flow. This can be seen by comparing frames at 7 and 8 min in Fig. 2C, between which the clot area reduction was almost twofold (from 55% to 27% of FOV). In addition, the increase of clot transparency was significant as well, indicating the removal of a large flat clot fragment in the time interval between the frames. In real time, partly detached clot fragments often vibrated in the streaming plasma before they were torn off the remaining clot.

Image analysis of the remaining clot

Recorded microscopy image sequences of clots during thrombolysis were analyzed in the form of clot dissolution curves, i.e., normalized non-lysed blood clot areas as a function of time. Typical examples of these (single experiment) curves, two corresponding to slow flow and the other two to faster flow of plasma containing rt-PA, are depicted in Fig. 3A. The curves indicate that thrombolysis on the microscopy scale runs in discrete steps of consecutive removal of superficial clot fragments. Each leap in the curve with 15 s time-resolution could be attributed to the removal of at least one clot fragment. Fig. 3B shows the sequential non-lysed clot area change as a function of time, i.e., a dissolution curve derivative (a plot of differences between sequential points of the graph in Fig. 3A), for both slow and faster flow of the two experiments from Fig. 3A depicted with big symbols. The largest area removed was approximately four times larger with faster than with slow flow (149,000 μm^2 vs. 35,000 μm^2).

Clot dissolution curves of individual clots were averaged for each experimental regime, thus obtaining the six averaged clot dissolution curves shown in Fig. 4. The initial transport time of rt-PA from the reservoir to the clot was 20 s with slow flow and 2 s with faster flow. Three of the curves (with void symbols), which correspond to control experiments with no rt-PA, overlap and are equal to unity throughout the experiment, indicating no clot dissolution. Addition of rt-PA to plasma in all experimental regimes resulted in changes of the clot dissolution curves. In the absence of flow (no perfusion experiment, blue curve) the clot area increased by 4% by the end of the experiment. In both rt-PA perfusion experiments the averaged clot dissolution

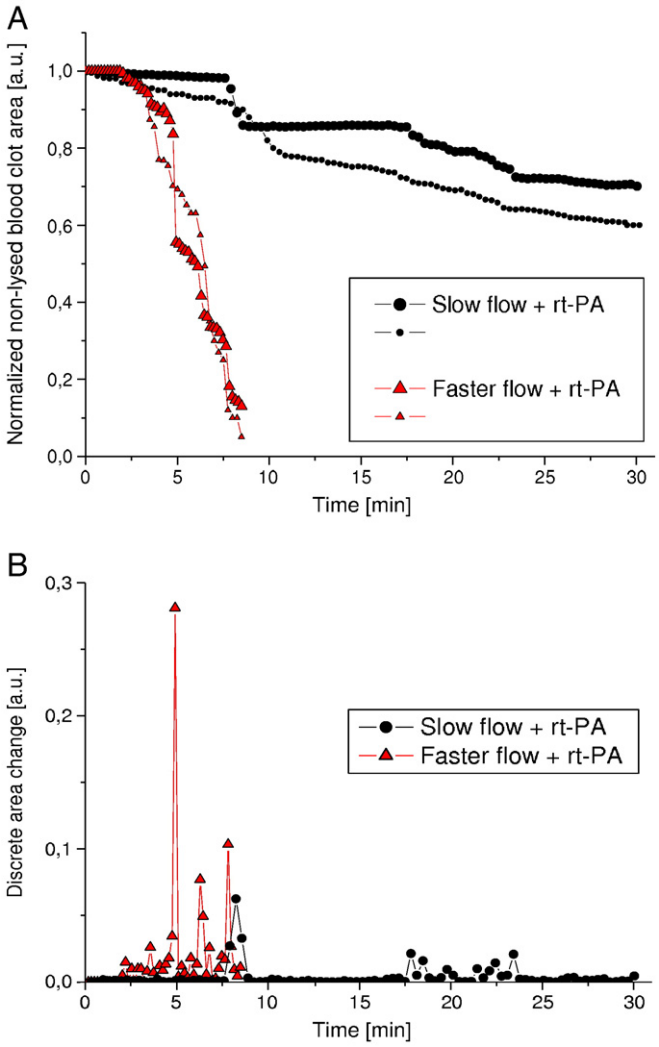

Fig. 3. Clot dissolution curves (A) and the corresponding sequential area changes (B) for individual representative rt-PA-mediated experiments; with slow flow (circles) and with faster flow (triangles). The graphs show flow-dependent clot dissolution dynamics that progresses as loss of clot area in discrete steps (A) with corresponding peaks denoting the size of discrete area changes as a function of time (B). Note that the curves in graph (B) are the first derivative of curves in graph (A, big symbols). Each step or peak in the curves corresponds to at least one removed clot fragment.

curves showed significant clot dissolution that was approximately five times faster with faster flow (red curve) than with slow flow (black curve); i.e., 50% dissolution was obtained in 6.5 min with faster flow, while more than 30 min was needed for 50% dissolution with slow flow. The normalized clot sizes differed significantly at 6.5 min ($P<0.05$). At the end of the lysis experiments, the average non-lysed blood clot area with faster flow amounted to 12% of the FOV at 8.5 min, and with slow flow to 55% of the FOV at 30 min. In addition, quantitative analysis of rt-PA mediated perfusion experiments is presented in Table 1 by absolute values of averaged non-lysed blood clot areas in selected representative times after thrombolysis beginning.

Distribution of removed clot fragment areas

The distribution of area changes, which was used as an estimate of the largest removed clot fragment, is presented in Fig. 5. The distribution comprises discrete area changes combined of all equivalent experiments. The area changes per 15 s frame rate were larger with faster flow than with slow flow. Both the average and the largest area changes differed; the average area change per 15 s was

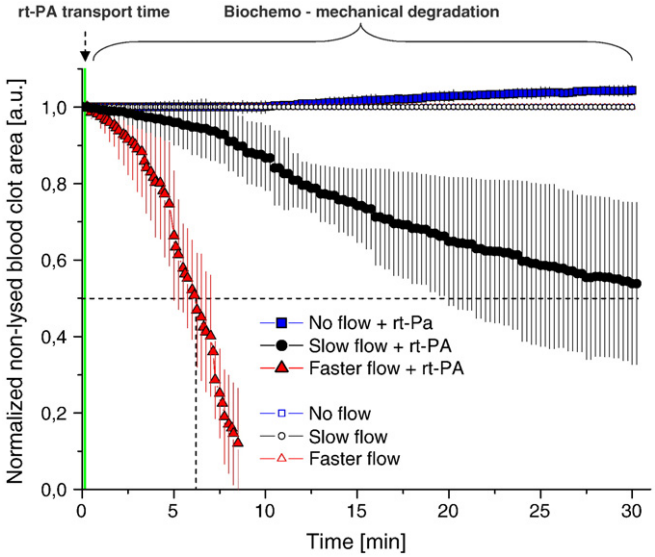

Fig. 4. Averaged dissolution curves, that show the normalized non-lysed blood clot area as a function of time, were obtained by averaging of at least five individual experiments of six different experimental regimes: rt-PA mediated (solid symbols) and control (without rt-PA, void symbols) each for slow (circles) and faster flow (triangles) perfusion, and the non-perfusion mode (squares). The dissolution curves of the all three control experiments (without rt-PA, void symbols) overlap as they are equal to unity. Mean values +/- standard deviation are shown. Vertical dashed line at 6 min designates 50% reduction of the initial clot area in FOV with the faster flow and rt-PA mediated thrombolysis.

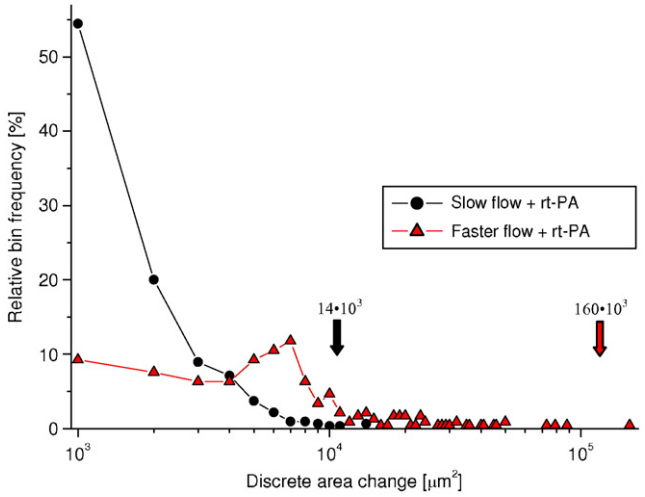

Fig. 5. Normalized distribution of sequential area changes at 15 s intervals in rt-PA mediated thrombolysis with slow (circles) and faster flow (triangles); bin size is equal to 1000 μm². The largest discrete area change in slow and faster flow had areas of 14,000 μm²and 160,000 μm², respectively. The distribution comprises discrete area changes combined of all equivalent experiments.

2200 μm² with slow flow vs. 10,600 μm² with faster flow, while the corresponding largest area changes were 14,000 μm² with slow flow vs. 160,000 μm² with faster flow. Differences in area changes between the two flow regimes were significant ($P<0.05$ by Mann-Whitney test). The distribution was normalized to the total number of area changes analyzed (720 with slow flow and 220 with faster flow).

Discussion

The aim of this study was to investigate the impact of mechanical forces of flowing plasma on the promotion of rt-PA-mediated thrombolysis of non-occlusive retracted whole blood clots. Our principal findings are that clot degradation cannot be initiated without a plasminogen activator by plasma flow alone, while in the presence of rt-PA and flow thrombolysis progresses by removal of microscopically visible clot fragments of flow-dependent sizes (ranging from 7 μm to 400 μm in diameter).

In the case of flowing plasma, shear forces appear due to plasma viscosity. In our experiments the shear forces were initially equal to 2.1 dyn/cm² and 21 dyn/cm² in slow and faster flow [7], respectively,

Table 1
Absolute averaged non-lysed blood clot areas in selected representative times after thrombolysis begining.

Time (min)	Non-lysed blood clot area (10^3 μm²)	
	Slow flow	Faster flow
0	519 ± 1	519 ± 1
2	513 ± 11	487 ± 39
4	503 ± 24	417 ± 74
6	492 ± 37	271 ± 66
8	472 ± 40	89 ± 67
10	450 ± 44	
15	385 ± 50	
20	337 ± 87	
25	304 ± 110	
30	279 ± 110	

and were gradually diminishing due to the decrease of plasma velocity (up to 25%) associated with the reduction of the clot profile during thrombolysis. Shear forces deform the clot and could potentially lead to its disintegration without any proteolytic action. However, the control experiments (Fig. 4, perfusion without rt-PA, void symbols) did not show any clot degradation with velocities up to 30 cm/s. The measured 4% clot area increase in no perfusion experiments was most likely due to intake of plasma with rt-PA and local chemical degradation associated with superficial swelling of the clot. The inefficient clot degradation can be explained by the extraordinary elastic properties of the fibrin meshwork [17,18], despite the fact that it represents only up to 1% of the clot's volume [14]. Addition of rt-PA initiates the biochemical component of fibrin degradation. The fibrinolytic process is dependent on the temperature [19], the concentrations of fibrinolytic reagents and the efficiency of their transport into the clot [18,20]. The mechanisms of molecular transport into clots are perfusion and diffusion, with perfusion being several orders of magnitude more efficient than diffusion alone [7,12].

Significant changes in the dissolution curves were obtained when the flow regime was changed from slow to faster. The changes can be attributed to better clot permeation with rt-PA [15] and to larger mechanical forces of the streaming plasma exerted on the clot surface [6]. Both result in more frequent and on average larger clot fragments being removed from the clot surface and therefore in more efficient thrombolysis.

Retracted whole blood clots were chosen as a model of non-occlusive venous thrombi, adhering to the vessel wall. The low susceptibility of retracted whole blood clots to thrombolysis in the absence of flow [15] was confirmed, since no retreat of the clot boundary was seen in 30 min when plasma contained rt-PA but was not flowing. Under these conditions the clot boundary moved outwards which can be explained by loosening of the clot after partial fibrin meshwork degradation. Efficient thrombolysis was only obtained with the combination of flow and the presence of rt-PA. The rheological conditions in our experiments were similar to those in the venous circulatory system [21]. The flow was steady and laminar; since the Reynolds number was 20 in the slow flow (3 cm/s) and 200 in faster flow (30 cm/s). Although systemic thrombolysis is rarely used for treating isolated venous thrombosis, it may be the treatment of choice in haemodynamically significant pulmonary embolism [1]. Pulmonary emboli undergoing thrombolysis may be exposed to similar flow conditions as in our faster flow regime and to a similar

plasma concentration of rt-PA. Also, the time scale of thrombolytic treatment of pulmonary embolism is similar to the duration of our experiments. We therefore believe that our experimental data, although primarily intended as a proof of a principle, may already have some physiological relevance, e.g., in explaining why thrombolytic treatment of pulmonary embolism works so poorly in patients who are in obstructive shock and cannot generate adequate flow through the pulmonary circulation.

Optical microscopy was chosen as the observation method since it provides good resolution at the micrometer level and allows for real time image acquisition. Due to its longer image acquisition times MRI microscopy [6,22] is not suitable for measuring fast processes, such as fragmentation of the clot boundary under flow conditions. On the other hand, MRI provides 3-dimensional information on the structure of the investigated objects, while conventional optical microscopy is limited to 2-dimensional images. The study could be improved by the use of confocal microscopy, which can provide 3-dimensional images of the surface in a rapid sequence. Confocal microscopy was already employed in non-perfusion thrombolytic experiments of fibrin clots without blood cells [10].

Traditionally, fibrin degradation products have been characterized biochemically by gel electrophoresis [23] or by immunological detection of D-dimer [24]. These methods characterize fibrin degradation products at the molecular level, but as our study clearly demonstrates, thrombolysis under flow conditions is not a purely biochemical process, as it proceeds via sloughing of clot fragments ranging in size from the micrometre to the millimetre scale. A possible future improvement of our study would be correlating the plasma D-dimer levels with clot morphology and hemodynamic conditions during thrombolysis.

A limitation of the study was the inability to detect small clot fragments travelling with faster plasma flow. This was a consequence of the limited speed and sensitivity of the microscope digital camera, which yielded optimal results at an exposure time of 20 ms. Continuous filming at that exposure time, i.e., with 50 fps, would not overcome the detection problem of moving clot fragments. To obtain sharp images of the moving clot fragments in faster flow (30 cm/s) or at velocities mimicking arterial flow conditions, an ultrafast camera with exposure times in the μs range would be needed. Fortunately, the inability to visualize directly the rapidly moving clot fragments was at least in part overcome by analyzing the discrete area changes in the clot surface and thus estimating the upper limit of the removed fragment sizes. In principle, all discrete changes in the remaining clot size could be attributed to one or more removed fragments (see Fig. 2.) As Fig. 5 shows, the most frequent events were small discrete area changes, with the frequency of these events being inversely proportional to the size of the discrete area change. Therefore, the probability of removing several large fragments in a single time frame was lower than that of removing several small or medium size clot fragments, and the largest discrete area changes could be most likely attributed to a single removed clot fragment. If the graph in Fig. 5 showed the removed fragment area distribution rather than the discrete changes in the remaining clot size, then the faster flow curve would be expected to have a similar decaying shape as the slow flow curve, without the shoulder at 7000 μm^2 that probably represented the sum of areas of multiple smaller clot fragments.

All the blood flow-associated phenomena have an increasing impact on the mechanical clot degradation with increasing flow velocities. Flow velocities in the largest human arteries can exceed 1 m/s, which is three times more than the flow velocity in our faster flow regime, and flow velocities in narrowed arteries can reach several m/s. Another important factor, that has an impact on mechanical clot degradation is the vessel diameter. Namely, in larger vessels, especially at the site of stenosis, occurrence of turbulent flow is likely. Mechanical forces of streaming blood on the surface of the clot are much higher in turbulent flow than in laminar flow, therefore promotion of thrombolysis is expected with flow velocities above the threshold for the turbulent flow regime, i.e., when the Reynolds number exceeds 3000 [6]. It would be interesting to perform in vitro experiments with rapid arterial-like flow, but such experiments are technically difficult due to the confined geometry of the observation chamber in which turbulent flow is unlikely to develop.

In summary, thrombolysis of retracted whole-blood clots *in vitro* is a biochemical and mechanical process in which the mechanical forces of the streaming plasma act in conjunction with the biochemical fibrinolytic reactions leading to efficient thrombolysis, while each process alone is inefficient. Optical microscopy showed that thrombolysis under flow conditions progresses in discrete steps of fragment sloughing from the clot surface. The size of clot fragments and the frequency of their removal increase with increasing tangential plasma flow velocity.

Conflict of interest statement

Details of nature of conflict of interest: No conflicts.

Acknowledgements

We thank Dr. Dragoslav Domanovič from the Blood Transfusion Centre of the Republic of Slovenia for kindly providing human plasma no longer intended for use in humans.

References

[1] Stashenko GJ, Hargett CW, Tapson VF. Thrombolytic therapy for venous thromboembolism: current clinical practice. J Hosp Med 2009;4:313–6.
[2] White-Bateman SR, Schumacher HC, Sacco RL, Appelbaum PS. Consent for intravenous thrombolysis in acute stroke: review and future directions. Arch Neurol 2007;64:785–92.
[3] Jenkins PO, Turner MR, Jenkins PF. What is the place of thrombolysis in acute stroke? A review of the literature and a current perspective. Clin Med 2008;8:253–8.
[4] Comerota AJ, Gravett MH. Do randomized trials of thrombolysis versus open revascularization still apply to current management: what has changed? Semin Vasc Surg 2009;22:41–6.
[5] Collen D. The plasminogen (fibrinolytic) system. Thromb Haemost 1999;82:259–70.
[6] Sersa I, Vidmar J, Grobelnik B, Mikac U, Tratar G, Blinc A. Modelling the effect of laminar axially directed blood flow on the dissolution of non-occlusive blood clots. Phys Med Biol 2007;52:2969–85.
[7] Wootton DM, Popel AS, Alevriadou BR. An experimental and theoretical study on the dissolution of mural fibrin clots by tissue-type plasminogen activator. Biotechnol Bioeng 2002;77:405–19.
[8] Pleydell CP, David T, Smye SW, Berridge DC. A mathematical model of post-canalization thrombolysis. Phys Med Biol 2002;47:209–24.
[9] Anand S, Diamond SL. Computer simulation of systemic circulation and clot lysis dynamics during thrombolytic therapy that accounts for inner clot transport and reaction. Circulation 1996;94:763–74.
[10] Sakharov D, Nagelkerke JF, Rijken DC. Rearangements of the fibrin network and spatial distribution of fibrinolytic components during plasma clot lysis. J Biol Chem 1996;26:2133–8.
[11] Grobelnik B, Vidmar J, Tratar G, Blinc A, Sersa I. Flow-induced permeation of non-occlusive blood clots: an MRI study and modelling. Eur Biophys J 2008;37:1229–33.
[12] Blinc A, Francis CW. Transport processes in fibrinolysis and fibrinolytic therapy. Thromb Haemost 1996;76:481–91.
[13] Šabovič M, Lijnen HR, Keber K, Collen D. Correlation between progressive adsorption of plasminogen to blood clots and their sensitivity to lysis. Thromb Haemost 1990;64:450–4.
[14] Blinc A, Keber D, Lahajnar G, Zupancic I, Zorec-Karlovsek M, Demsar F. Magnetic resonance imaging of retracted and nonretracted blood clots during fibrinolysis in vitro. Haemostasis 1992;22:195–201.
[15] Tratar G, Blinc A, Strukelj M, Mikac U, Sersa I. Turbulent axially directed flow of plasma containing rt-PA promotes thrombolysis of non-occlusive whole blood clots in vitro. Thromb Haemost 2004;91:487–96.
[16] Colman RC, Hirsch J, Marder VJ, Salzmna E, editors. Haemostatis and thrombosis. Basic principles and clinical practice. Philadelphia: JB Lippincitt Co; 1994.
[17] Liu WJLM, Sparks EA, Falvo MR, Hantgan RR, Superfine R, Lord ST, et al. Fibrin fibers have extraordinary extensibility and elasticity. Science 2006;313:634.
[18] Weisel JW. Structure of fibrin: impact on clot stability. J Thromb Haemost 2007;5(Suppl 1):116–24.

[19] Shaw GJ, Dhamija A, Bavani N, Wagner KR, Holland CK. Arrhenius temperature dependence of in vitro tissue plasminogen activator thrombolysis. Phys Med Biol 2007;52:2953–67.
[20] Ruggeri ZM. Mechanisms initiating platelet thrombus formation. Thromb Haemost 1997;78:611–6.
[21] Stein PD, Yaekoub AY, Ahsan ST, Matta F, Lala MM, Mirza B, et al. Ankle exercise and venous blood velocity. Thromb Haemost 2009;101:1100–3.
[22] Tratar G, Blinc A, Podbregar M, Kralj E, Balazic J, Sabovic M, et al. Characterization of pulmonary emboli ex vivo by magnetic resonance imaging and ultrasound. Thromb Res 2007;120:763–71.
[23] Marder VJ, Francis CW. Plasmin degradation of cross-linked fibrin. Ann N Y Acad Sci 1983;408:397–406.
[24] Adam SS, Key NS, Greenberg CS. D-dimer antigen: current concepts and future prospects. Blood 2009;113:2878–87.